

PREDICTION OF AEROELASTIC EFFECTS OF AIRCRAFT CONFIGURATIONS INCLUDING HIGH LIFT SYSTEMS

K. C. Chang, H. H. Chen, T. Tzong and T. Cebeci
The Boeing Company, Long Beach, CA

Keywords: *Aeroelasticity, CFD, Structure, Finite-element Model, High-lift System*

Abstract

An interface method for coupling aerodynamics and structures has been developed. The method transforms loads computed by any aerodynamic code to structural finite element (FE) model based on virtual work and converts displacements from the FE model to aerodynamic grid points on the aircraft surface through the reciprocal theorem in structural engineering. The method was used to evaluate the aeroelastic effects for an advanced transport wing at cruise, under-cruise and stall conditions. Results, in good agreement with wind tunnel data, show a pronounced influence of aeroelasticity on the aerodynamic performance of the wing. The method was also applied to more complicated configurations including an MD90 wing/ fuselage configuration, a simple three-element high lift system, and a rather complicated high lift system of an advanced high-wing transport aircraft. Results show that the interface method also works well for all these complex configurations.

1 Introduction

The aeroelastic analysis of an aircraft requires an accurate and efficient procedure to couple aerodynamics and structures. Either a closely coupled approach or a loosely coupled approach could be adopted. In a closely coupled approach, the aerodynamic and structural equations are solved simultaneously. In a loosely coupled approach, the loads computed with an aerodynamic model are transformed into a structural model for structural analysis, and the displacements resulting from the

structural analysis are converted back to the aerodynamic model to update the geometry. The advantage of the closely coupled approach is that the results can be obtained with a single analysis. However, extensive code modification is required to couple structural and aerodynamic codes and, hence, the evaluation of a new structural or aerodynamic code may be time-consuming and costly. On the contrary, a general interaction procedure using the loosely coupled approach can be developed at a cost of a few iterations between aerodynamic and structural models to get converged solutions for loads and displacements. Using this procedure, the aeroelastic analysis can be conducted using any aerodynamic and structural codes with little modification to either code.

It is always the desire of aerodynamic engineers and loads engineers to perform aerodynamic calculations and compute loads using high-fidelity aerodynamic and structural models. In such a way, accurate pressure and load distributions on the wing and its components such as flaps, slats and spoils can be predicted including aeroelastic effects. An interface method using a loosely coupled approach has been developed to satisfy needs of both engineers[1-4]. This method is general in the sense that the loads computed by any aerodynamic code can be transformed to the finite element (FE) model and displacements can be transformed from the FE model to the aerodynamic model.

After a description of the interface method in Section 2, it is validated with an advanced transport wing at cruise, under-cruise and stall conditions. Using the parallel version of the OVERFLOW code[5] to compute the

aerodynamic loads and a finite element code to perform structural analysis, the aeroelastic effects for this wing are calculated and the results are compared with the experimental data in Section 3. The application of the interface method to wing/fuselage configurations is presented in Section 4 with an MD90 wing/fuselage configuration is chosen for this purpose. The application to high lift systems is given in Section 5. Results for a simple three-element high lift system are discussed in details. The method is also applied to a rather complicated high lift system of an advanced high-wing transport aircraft. The aerodynamic loads for the high lift systems are calculated by Hess panel method[6]. This paper ends with conclusions in Section 6.

2 Interface Method

A general interface method must be able to take into account of the different characteristics between aerodynamic and structural models in order to convert the loads and deformations between the two models. The aerodynamic model generally includes details of the aircraft geometry, such as flaps, slats, pylon, nacelle, etc., and closely resembles to the true geometry of the aircraft. However, the structural finite element model is usually represented only by major structural components. For example, the wing box, which carries major loads, is of main structural concern and is modeled in detail. The flaps and slats, which carry relatively small loads, are either represented by simple beam elements or completely excluded from the FE model. In addition, engine and pylon usually modeled by a lumped (point) mass element and a general stiffness matrix, respectively, which do not resemble the true configurations of the components at all. Furthermore, tens of thousands aerodynamic grid points on the surface of an aircraft are usually needed to compute the pressure distribution. However, only hundreds or thousands of FE nodal points are used to model aircraft structures. The difference in fidelity results in gaps between the aerodynamic and the FE models. In order to accurately convert the loads and displacements,

the difference between the two models must be considered in the interface method.

A general interface method that fulfills the above requirements has been developed[1-4]. This method is based on FE technology in which virtual work is employed to transform aerodynamic pressures into FE nodal forces. The displacements at FE nodes are then converted back to aerodynamic grid points on the aircraft surface through the reciprocal theorem in structural engineering. The conversion of loads between the aerodynamic and FE models is accomplished by integrating pressures on the aerodynamic model rather than transforming the pressures directly to the FE model. The reason for this choice is that the surface area of the FE model does not represent the aircraft geometry accurately.

The first step in performing the aeroelastic analysis with the interface method is to project each aerodynamic grid point on the aircraft surface onto an adjacent finite element. The projection generates basic data needed in the aero-structure interaction process. The data include the finite element projected by each aerodynamic grid point, the projected location of the aerodynamic grid point on the element and the offset distance from the aerodynamic grid point to the element surface.

With this information, the displacements at an aerodynamic grid point on the aircraft surface can be expressed in terms of displacements at the projected location on the finite element surface as

$$\underline{u}_{aero} = \frac{1}{2} \begin{bmatrix} 1 & 0 & 0 & 0 & r_z & 0 \\ 0 & 1 & 0 & -r_z & 0 & 0 \\ 0 & 0 & 1 & 0 & 0 & 0 \end{bmatrix} \nabla \begin{Bmatrix} u \\ v \\ w \end{Bmatrix}_{FE} \quad (1)$$

where \underline{u}_{aero} contains three translational displacement components at the aerodynamic grid point, and r_z is the offset distance from the grid point to the projected finite element, and

$$\nabla = \begin{bmatrix} 2 & 0 & 0 & 0 & \partial/\partial z & -\partial/\partial y \\ 0 & 2 & 0 & -\partial/\partial z & 0 & \partial/\partial x \\ 0 & 0 & 2 & \partial/\partial y & -\partial/\partial x & 0 \end{bmatrix}^T.$$

Since the aircraft surface is usually modeled by membrane elements, which do not have rotational degrees of freedom (DOF), the FE displacements only include the translational DOF, u , v and w .

With the introduction of the FE shape functions, the translational displacements at any location on the element surface can be written as

$$\bar{u}_{FE} = \underline{N}\underline{U} = \sum_i \begin{bmatrix} N_i & 0 & 0 \\ 0 & N_i & 0 \\ 0 & 0 & N_i \end{bmatrix} \begin{Bmatrix} U \\ V \\ W \end{Bmatrix}_i \quad (2)$$

The aerodynamic grid displacements then become

$$\underline{u}_{aero} = \underline{G}\underline{U}_{FE} \quad (3)$$

where \underline{G} is the combination of matrices of transformation, differential operators and FE shape functions.

By employing the reciprocal theorem, finite element nodal forces are written in terms of forces at the aerodynamic grid point as

$$\underline{P}_{FE} = \underline{G}^T \underline{P}_{aero} \quad (4)$$

where \underline{P}_{FE} is the finite element force vector and

$$\underline{P}_{aero} = \left\{ \begin{matrix} p_x & p_y & p_z \end{matrix} \right\}_{aero}^T$$

is the force at the aerodynamic grid point obtained by integrating aerodynamic pressures over the area surrounding the point. In the above equation, the moments due to the offset distance r_z from the aerodynamic grid point to the element surface and the in-plane force components p_x and p_y are conserved. In addition, the aerodynamic forces on aircraft components that are excluded from the finite element model can be properly transformed.

The finite element load vectors are computed by virtual work as

$$W = \int \delta \underline{u}_{FE}^T \underline{P}_{FE} dA = \delta \underline{U}^T \underline{F} \quad (5)$$

Here W is the virtual work, \underline{P}_{FE} and \underline{u}_{FE} are the force and displacement vectors at any point on the element surfaces, and A is the surface area of the structure. \underline{F} and \underline{U} are the finite element nodal loads and displacements, respectively.

After the load vector is formed, the displacements at finite element nodes can be obtained by structural analysis. The displacements at aerodynamic grid points are computed by Equation (3). Details of the derivation for the interface method can be found in Ref. 1.

The interface method described above was originally developed for simple configurations like wing and wing/ fuselage. It, however, must be enhanced in order to compute aeroelastic effects of complicate geometry such as wing/nacelle/strut/ engine and high-lift systems. As discussed in Ref. 1, the projection of the aerodynamic grid point onto a finite element is selected based on two criteria (1) the closest finite element and (2) the least extrapolation of FE surface projection. If both criteria are satisfied by more than one element, the interfacing cannot proceed properly. The difficulty of applying the method to complicated geometry resides in areas where aerodynamic grid points could be projected onto multiple structural components, for example, the gaps between the slat and main wing. When more than one element from different components meet the criteria, the interface method may select an element that is not on the desired component and, hence, will not generate a smooth deformed shape of the aerodynamic grid. Consequently, the pressure distribution from the next aerodynamic calculation will not be accurate.

To resolve this problem, the interface method is enhanced. The aerodynamic and structural models are divided into different zones. In each zone, the projection of aerodynamic grids is limited to finite elements within the same zone. For example, a leading edge slat can be a zone. Therefore, the aerodynamic grids on the slat can only be projected onto the finite elements composing the slat. There are two advantages of using the

zonal approach: (1) the logic of searching the “right” FE for each grid point is the same as the original method for a single component, and (2) the computing time for locating the element is reduced. Using this zonal approach, the interface method can be applied to any complicated geometry with minor additional efforts to define the zones.

One of the major problems of computational fluid dynamics (CFD) in solving the Euler/ Navier-Stokes equations lies in the area of grid generation, which can be tedious and labor-intensive. For aeroelastic analysis, iterations between the aerodynamic and structural models are required to get converged solutions for both loads and deformations. To generate a new grid of the deformed geometry for every iteration can involve substantial work, which may not be practical and acceptable. To minimize the effort, a grid perturbation technique for moving grids is desirable for the aeroelastic calculations.

A grid perturbation code, CSCMDO, developed by Jones & Samareh-Abolhassani[7] at NASA Langley, was adopted for this purpose. This code generates a new grid for the deformed geometry by perturbing the original grid such that the surface of the new field grid coincides with the surface of the deformed geometry. It is applicable as long as the movements of the deformed surface are small so that the original grid topology is not violated. The code can be used for grid systems with either single or multiple blocks.

CSCMDO can be used to generate grids to solve either the Euler or Navier-Stokes equations. For the latter, care must be taken to satisfy the requirement of extremely fine grid spacing near the wall. This makes the grid perturbation difficult. For complex geometries such as the MD90 wing/fuselage configuration, the grid perturbation code is not capable of generating the Navier-Stokes grid for the deformed geometry directly. Instead, the code is first used to perturb the Euler grid in which coarser grid spacing near the wall is allowed. The perturbed Euler grid is then adjusted to satisfy the grid requirements for Navier-Stokes calculations.

3 Validation and Evaluation

To validate the aero-structure interface method, static aeroelastic analysis was performed on an advanced transport wing model for which extensive wind tunnel data are available. This model[8] is a 2.426 percent scale representation of the original advanced transonic transport configuration, MD12. The wind tunnel tests were conducted at the NASA Langley National Transonic Facility (NTF). The model was made of solid metal with cutouts under the wing along the span and additional cutouts in the outboard region for installation of measuring equipment. The wing geometry was designed and fabricated with a model jig twist distribution which will deform under load to the correct “1-G” twist at $M_\infty = 0.85$ and $C_L = 0.60$ [8].

The finite element model of this wing is composed of 5937 nodes, 6705 elements and 17508 degrees of freedom, as shown in Figure 1. Eight-node solid hexagon elements are used to model the wing structure. The finite element nodes were carefully defined on the plane of wing sections to maintain the bending characteristics of the wing. Moreover, all cutouts on the wing and the separation between the wing and its tip control surface were included in the model.

Calculations were performed for cruise, under-cruise and stall conditions for $M_\infty = 0.85$ and $Re = 4.3 \times 10^6$ based on the mean aerodynamic chord. The pressure distributions were computed by the parallel version of the OVERFLOW code[5] with the Baldwin-Barth turbulence model on IBM SP-2. A C-O type field grid containing $321 \times 81 \times 49$ grid points was used in the calculations. The grid system was partitioned into five blocks to facilitate the distributed processing on IBM SP-2. The grid perturbation code, CSCMDO, was used to generate the deformed grid for every iteration.

For the cruise condition with $\alpha = 1.7^\circ$, Figure 2 shows the undeformed and deformed wing geometry based on the aerodynamic model. Figure 3 shows the pressure distributions at four different spanwise locations for both the undeformed and deformed wings

with the experimental data. As can be seen, the shock location moves forward and the suction peak changes drastically in the outboard region as the wing deforms. The predicted pressure distributions on the deformed wing are in good agreement with the experimental data. Also, the shock location and strength are captured well in the numerical solutions. The good agreement with data demonstrates that the present aero-structure interface method functions well and gives accurate results. The calculated results also indicate the significance of the aeroelastic effects. Results for under-cruise conditions with $\alpha = 1.1^\circ$ and at stall conditions also show that the predicted pressure distributions on the deformed wing are in good agreement with the experimental data and the shock location and strength are also well captured.

4 Application to MD90 Wing/Fuselage Configuration

The interface method is applied to an MD90 wing/fuselage configuration. The original structural model of this configuration contains a wing box and a fuselage barrel near the wing root area. The fuselage barrel was extended to include the cockpit and tail sections by adding a series of beam elements at the center of fuselage. In order to convert loads from the aerodynamic model to the structural model, dummy membrane elements (with zero stiffness and mass) were used to model the fuselage surface. The loads on the membrane elements are transformed to the center beam elements through rigid elements, which form a wagon wheel shape at each fuselage cross section as shown in Figure 4. The skin, ribs and spars in the wing box were modeled by membrane elements and stringers modeled by beam and rod elements. Additional dummy membrane elements were added to the leading and trailing edges of the wing in order to convert loads properly from the aerodynamic model into the FE model. The FE model contains 5,748 nodes, 14,518 elements and 32,931 degrees of freedom. Two points on the plane of symmetry of the wing/fuselage configuration are fixed to allow the bending deformation of the fuselage.

The pressure distributions on the surface of the MD90 wing/fuselage at the cruise conditions with $M_\infty = 0.76$ and $\alpha = 2^\circ$ were again computed by the parallel version of OVERFLOW code with the Baldwin-Barth turbulence model. The grid was of the C-O type field grid containing $289 \times 73 \times 49$ grid points with 225×49 grid points on the wing surface and 267×25 grid points on the fuselage surface. And the grid system was again partitioned into four blocks to facilitate the distributed processing. The grid perturbation technique was used to reduce the grid generation work at every iteration.

Figure 5 shows the deformed and undeformed wing/fuselage geometry of the aerodynamic model. The smoothness of the geometry demonstrates that the aero-structure interface procedure functions well for wing/fuselage configurations. Figure 6 shows the pressure distributions at four different spanwise locations for both deformed and undeformed wing/ fuselage configurations. As can be seen, near the wing root, the aerodynamic pressures remain almost the same and the shock location only changes slightly. However, the shock location moves toward the leading edge and the suction peak becomes smaller in the outboard region as the wing deforms.

The calculations show that near the leading edge there is a dip in the pressure coefficient on both the upper and lower surfaces of the wing when the wing/fuselage configuration deforms. It is found that the dip is caused by the separation between the slat and the wing box due to structural deformation.

5 Application to High Lift Systems

The goal of this study is to investigate the aeroelastic effects on high lift systems of general aircraft configurations. An obvious choice for calculating aerodynamic loads on high lift systems is to use Navier-Stokes methods like the OVERFLOW described previously. However, high lift systems are very complex in both geometries and flow physics. The presence of high and low Reynolds number flows on various components of wing and

significant regions of flow separation on them well before stall conditions make accurate predictions of the flow difficult, if not impossible. The solution of the Navier-Stokes equations for high lift systems requires several millions grid points to appropriately resolve the flow field around the complex three-dimensional configurations, leading to high demands on computer resources and extensive grid generation effort. Furthermore, an aeroelastic analysis usually requires several iterations to reach a converged solution between the aerodynamic loads and the structural deformations. Therefore, in the present study, an alternative approach based on the interactive boundary layer (IBL) theory is used to calculate the aerodynamic loads. The IBL approach solves the inviscid flow, boundary layer and stability/transition equations interactively. It has been applied successfully to two- and three-dimensional flows[9,10] with results of similar quality to that of Navier-Stokes solutions at a cost barely exceeding that of the methods currently used in high lift design. As such, it provides a good compromise between the efficiency and accuracy required in a design process.

The AGARD A2 high lift system was generated by expanding the AGARD A2 high lift airfoil into a wing configuration with aspect ratio of 6.0, taper ratio of 0.35, leading-edge and trailing-edge sweep angles of 30 and 15 degrees, respectively. The aerodynamic performances of the system are expected to be close to the high lift systems used in most commercial aircraft.

Figure 7 shows the panel distributions of the A2 high lift system for the aerodynamic analysis, which consist of three sections and 3,300 panels. The finite element model of the system for the structural analysis is shown in Figure 8. The model is composed of membrane elements for skin, ribs and spars, and beam elements for stringers and actuators. Both the slat and the flap are divided into two portions, inboard and outboard, at the 50% span-wise location and each of them is connected to the main wing by two actuators. The arrangement allows separation between inboard and outboard

slats and flaps when differential deflections between them exist. Three zones including slat, main wing and flap are defined. The data for each zone include the aerodynamic grids and associated surface finite elements. Since the zone information is only for interface purpose, they do not affect the aerodynamic pressure calculation and the finite element analysis.

The aeroelastic effects for the flow conditions at Mach number of 0.3 and the angle of attack of 16.0° are shown in Figures 9 to 11. Figure 9 shows a comparison of the section lift distributions with and without aeroelastic effects. The effect of aeroelasticity on the reduction of the total lift coefficient is 0.06; this is equivalent to 2.0% of the total lift coefficient. The calculated vertical shift distributions and twist angle distributions due to the aeroelasticity are shown in Figures 10 and 11, respectively. A jump of twist angle for flap at about 50% span location reflects the separation of inboard and outboard flap in the finite element model. At the wing tip, the wing moves upward about 3.5% of the wing's semi-span, and the wing's cross section twists by about 1.3° . The values are in the range of the wind-tunnel measurements on the MD11 high lift configurations.

The interface method was also successfully applied to a rather complicated high-lift system of an advanced high-wing transport aircraft configuration. The configuration includes slat, main wing, flap, fuselage, strut, nacelle, and winglet. The aerodynamic model is composed of 20 sections and 10,865 grids and the FE model consists of 35,200 solid elements, 4,000 plate-shell elements and 58,600 nodes. (See Figs. 12 and 13) In the analysis, the entire model is grouped into 12 zones for interfacing and each zone has an associated FE surface mesh and an aerodynamic grid. The calculations run smoothly without any difficulty. Figure 14 shows the deformed and undeformed shapes of the aerodynamic model. Because of the restrictions on this configuration, no further detailed results are permitted to present here.

6 Conclusions

A general interface method has been developed to compute the aeroelastic effects on general aircraft configurations. The method was validated with an advanced transport wing at cruise, under-cruise and stall conditions. Calculated results also indicate the significance of aeroelastic effects on the aerodynamic performance of this wing.

The interface method was then applied to a MD90 wing/fuselage configuration at cruise conditions. The smoothness of the deformed geometry and similar results as the advanced transport wing mentioned above indicate that the interface method functions well for the wing/fuselage configurations.

The method was finally applied to two high-lift systems: an A2 high-lift system and a high-lift system of an advanced high-wing transport aircraft configuration. The A2 high lift system contains slat, main wing and flap. The predicted deformations are within the range of experimental observation of typical commercial aircraft configurations. The high-lift system of the transport aircraft is very complex and contains fuselage, slat, main wing, flap, strut, pylon, and winglet. There is no difficulty encountered in the calculations and the calculated deformed geometry is very smooth, indicating the method is also applied equally well to complex multi-component configurations.

References

- [1] Tzong, T., Chen, H. H., Chang, K. C., Wu, T. and Cebeci, T. A general interface method for aeroelastic analysis of aircraft. McDonnell Douglas Report No. MDC 96K7062, Feb. 1996.
- [2] Tzong, T., Chen, H. H., Chang, K. C., Wu, T. and Cebeci, T. A general method for calculating aero-structure interaction on aircraft configurations. AIAA-96-3982, 1996.
- [3] Chen, H. H., Chang, K. C., Tzong T. and Cebeci, T., Aeroelastic analysis of wing and wing/fuselage configurations. AIAA-98-0907, Jan. 1998.
- [4] Chang, K. C., Chen, H. H., Tzong, T. and Cebeci, T. Aeroelastic analysis of high lift configurations. AIAA-2000-0905, Jan. 2000.
- [5] Buning, P. G., Jespersen, D. C., Pulliam, T. H., Chan, W. M., Slotnick, J. P., Krist, S. E. and Renze, K., J. *OVERFLOW user's manual, version 1.7r*. NASA Ames Research Center, Moffett Field, CA, 1996.
- [6] Hess, J. The problem of three-dimensional flows and its solution by means of surface singularity distribution. *Computer Methods in Applied Mechanics and Engineering*, pp 283-319, 1974.
- [7] Jones, W. T. and Samareh-abolhassani, J. A grid generation system for multi-disciplinary design optimization. AIAA-95-1689, 1995.
- [8] Wilcox, P. A. Operating paper for the wind tunnel test of the 2.426% scale $M=0.85$ advanced transport model, LB-559D, in the NASA Langley research center national transonic facility (NTF). McDonnell Douglas Paper No. MDC 96K0203, Feb. 1996.
- [9] Cebeci, T., Bernard, E., and Chen, H. H. Calculation of multi-element airfoil flows including flap wells. AIAA-96-0056, Jan. 1996.
- [10] Bernard, E., Kural, O., and Cebeci, T. Flow predictions about three-dimensional high lift systems. AIAA-99-0543, Jan. 1999.

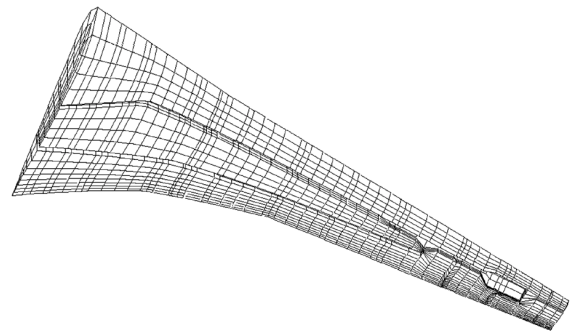
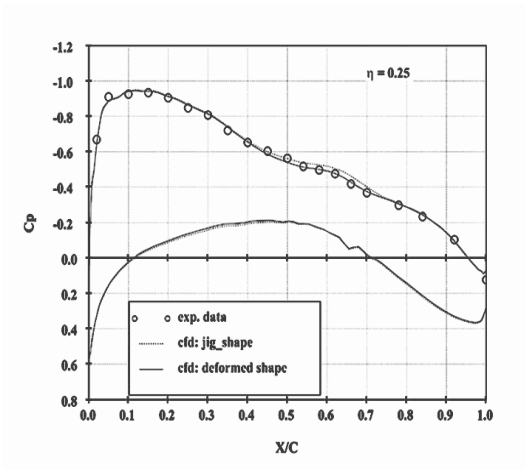


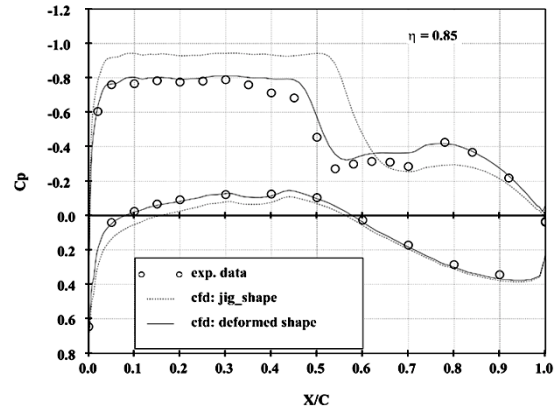
Fig. 1 The finite element model of the advanced transport wing



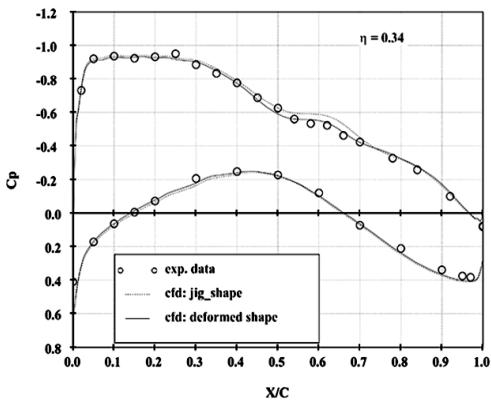
Fig. 2 The undeformed and deformed geometry of the advanced transport wing at the cruise condition



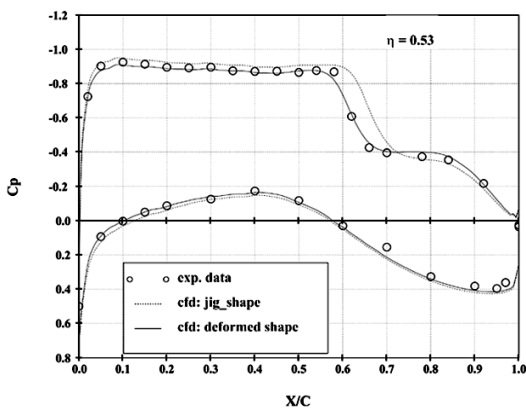
(a)



(d)



(b)



(c)

Fig. 3 The pressure distributions at four spanwise locations of the advanced transport wing at $\alpha = 1.7^\circ$

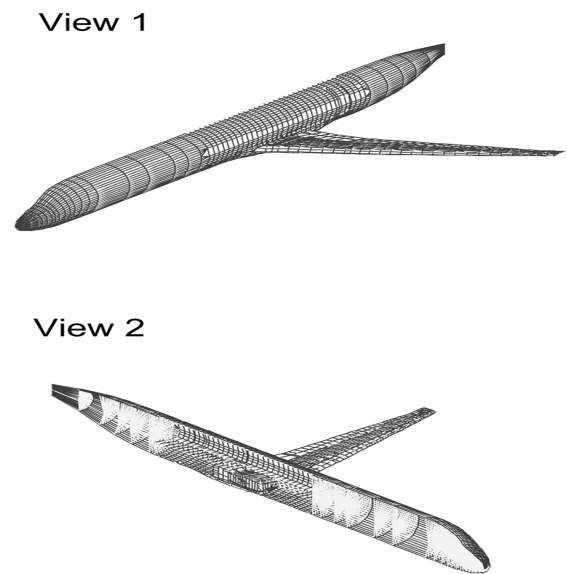


Fig. 4 The finite element model of the MD90 wing/fuselage configuration

PREDICTION OF AEROELASTIC EFFECTS OF AIRCRAFT CONFIGURATIONS INCLUDING HIGH LIFT SYSTEM

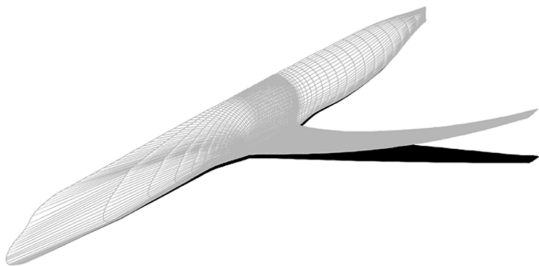
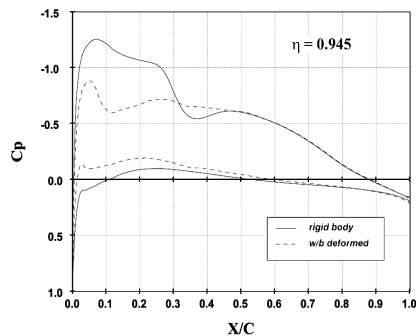
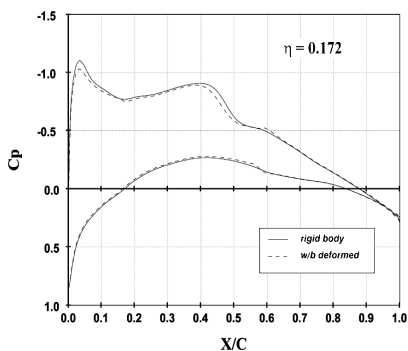


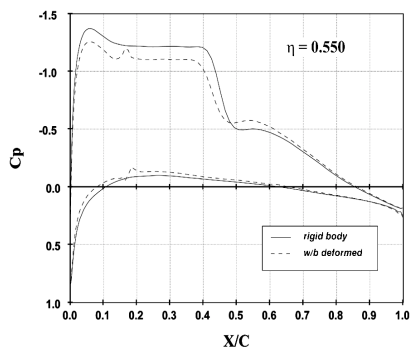
Fig. 5 The undeformed and deformed geometry of the MD90 wing/fuselage configuration



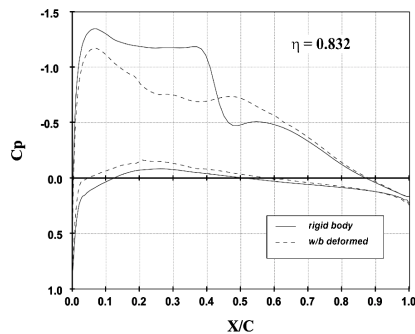
(d) Fig. 6 The pressure distributions at four spanwise locations of the MD90 wing/fuselage configuration



(a)



(b)



(c)



Fig. 7 Panel distribution of AGARD A2 wing



Fig. 8 Finite element model of AGARD A2 wing

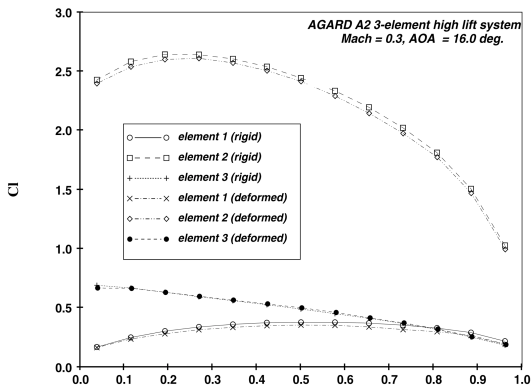


Fig. 9 Comparison of section C_L distributions: rigid vs. deformed

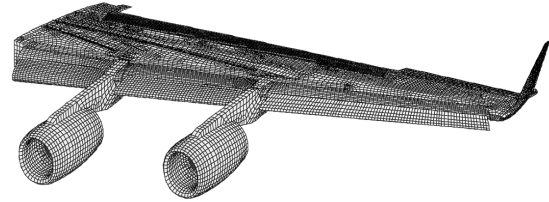


Fig. 12 Finite element model of the high-lift system of an advanced high-wing transport configuration

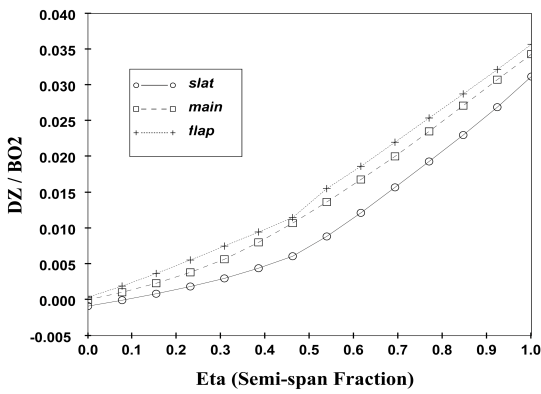


Fig. 10 Vertical shift (DZ) distributions due to aeroelastic effects for A2 high-Lift system

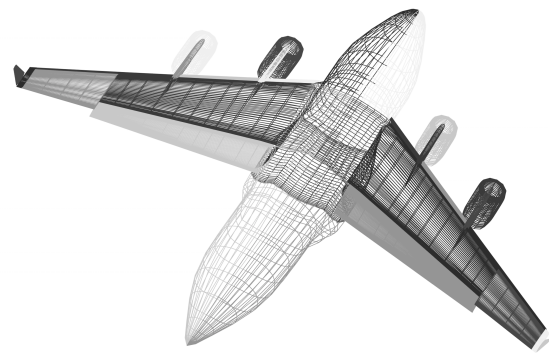


Fig. 13 Panel distribution of the high-lift system of an advanced high-wing transport configuration

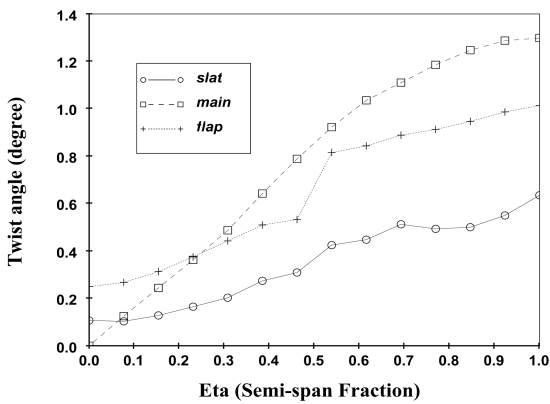


Fig. 11 Twist angle distributions due to aeroelastic effects for A2 high-lift system

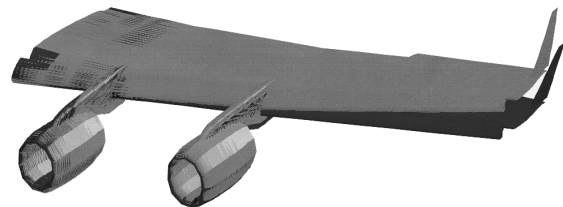


Fig. 14 Deformed and undeformed geometry of the aerodynamic model of an advanced high-wing configuration